System Architecture for Tracking Passengers inside an Airport Terminal Using RFID

Juan Jose Garau Luis, Bruce Cameron, Edward Crawley
Massachusetts Institute of Technology
77 Massachusetts Ave 33-409
Cambridge, MA 02139
617-682-6521
{garau, bcameron, crawley}@mit.edu

Marc Sanchez Net
Jet Propulsion Laboratory
4800 Oak Grove Dr
Pasadena, CA 91109
818-354-1650
marc.sanchez.net@jpl.nasa.gov

***Abstract*—Experts predict the number of devices connected to Internet of Things will reach 50 billion in 2020. In this paper, we apply the concept of IoT to the airport management industry and investigate the utilization of RFID technology to enhance airport mobility and security. We propose a system to track passengers inside an airport terminal and focus on the optimization of its architecture. To that end, we develop a simulation model incorporating the most important parts of the system, including: An airport model based on Chicago O'Hare International Airport, a passenger trajectory model, a link budget model, a coverage model, a reader placement algorithm, a communication protocol and the limitations of available RFID technology and regulations.**

Next, we identify a set of architectural decisions, such as the physical limits of the system or the specific technology to be deployed, and develop performance and cost metrics to compare the plausible architectures. Then, based on the developed model and the metrics space, we present the architectural tradespace of the system and analyze the impact each decision has in order to optimize the architecture. Finally, we assess the viability of the chosen architecture in terms of coverage and tracking performance.

TABLE OF CONTENTS

1. INTRODUCTION

Motivation

During this century, advancements in technology for storing, processing and transmitting data have led to the creation of new connectivity concepts such as Internet of Things (IoT). IoT is the creation of a digital replica from a physical object that provides real-time information about the state of the object. Given this simple but powerful concept, it is not surprising that numerous industries have included IoT in their workplans [1].

The aerospace sector is no exception to the adoption of IoT; in fact, the term Internet of Aerospace Things (IoAT) has recently become popular. IoAT aims to enhance connectivity in the aerospace domain to create a real-time feedback and control loop between systems and agents. Within the IoAT domain, this paper focuses on a system to track passengers inside an airport terminal by means of Radio Frequency Identification (RFID).

978-1-5386-2014-4/18/$31.00

An airport terminal is an environment where different agents coincide: Passengers, airport authority, pilots, crew, terminal workers, etc. Although each presents a different objective, two main goals stand out: Mobility and security. Regarding the former, passengers value short travel times and short queues at check-in counters, security points or boarding gates. At the same time, the airport authority is responsible for ensuring all the activity at the terminal is carried out securely.

Although there have been efforts to improve mobility and security in airport terminals, current solutions target specific locations (e.g. check-in counter, security gates). For instance, References [2] and [3] present models to optimize passenger queues and enhance airport security-checking technology. In contrast, we propose using RFID for crowd management [4] in large areas of the airport that comprise several of the key spots or locations of interest. In that sense, tracking passengers would provide real-time information to be used for waiting time estimation, service optimization and security management. This, in turn, would allow passengers to get recommendations on fastest routes or shortest queues, as well as let airport authority have data on passenger density at critical spots, so security agents could be allocated efficiently.

Research Goals

The main objectives addressed by this paper are:

1. Development of an airport model serving as the context of the system.
2. Determination of the set of feasible architectures and its RFID communications model.
3. Development of performance and cost metrics as architectural assessment criteria and posterior exploration of the architectural tradespace.
4. Optimization of the architecture of the system based on the impact of the architectural decisions.

Literature Review

Tracking people is a problem that has been extensively covered in the literature using different technologies such as LIDAR [5], RADAR [6], WiFi devices [7], and Computer Vision [8]. Tracking by means of passive RFID tags has also been a topic of research for trajectory analysis [9], information gathering [10], and people localization [11].

Although previous research has focused on a wide variety of environments, some studies also consider the use of RFID systems for tracking passengers inside airports. In [12], an RFID-based tracking system for airport security is presented, focusing on the software and hardware architecture of the Tag-Reader communication. This paper also explores how the different tag technologies affect the communication and assesses its operation under real airport conditions (at Athens International Airport). Their research demonstrated that it is feasible to use RFID tags attached to passengers' luggage to track them within the airport.

In [13], a patent, the applicability and advantages of using an RFID system for tracking passengers inside an airport are discussed. Without providing details on specific RFID technology or implementation, it proposes this method for solving some problems on mobility and security.

Finally, in [14] an RFID model designed to be used in airports for security and efficiency is presented. The work considers a cellular network of passive RFID receivers and far-field active RFID tags. It also considers the communication problems that may arise such as non line-of-sight conditions or multi-path fading.

Paper Structure

The remainder of this paper is structured as follows: In section 2 we start with a brief introduction to RFID, highlighting the specific features of the proposed system. Section 3 focuses on the modeling of the airport environment i.e., the terminal and the passengers, which serve as the shared context of the different system architectures. Next, in Section 4 we model the system, addressing the elements that draw its architectural differences. Section 5 is devoted to the description of the architectural decisions, the metrics adopted to evaluate the impact of each decision, and the tradespace exploration for all the considered architectures. Finally, the paper concludes with a summary of results and a discussion of lines of future work.

2. RFID AS CONCEPT

RFID Technology

RFID is an automatic identification procedure based on using electromagnetic waves for power supply and data-exchange with a data-storing device [15]. The basic RFID communication system has three different elements: A reader, a tag, and a wireless channel serving as the communication medium. Tags are usually attached to objects and, if within the reader's range, they can be detected and identified. We choose passive RFID tags for this study, as their batteryless architecture makes them ideal for large-scale deployments.

Regarding RFID readers, as in previous research studies [16][17], we focus on EPC Class-1 Generation-2 protocols (C1G2). According to C1G2 and US FCC regulations, RFID readers are only allowed to use fifty 500 kHz channels in the Ultra High Frequency (UHF) 902-928 MHz band. Furthermore, the maximum transmit power by an RFID reader is 1 W and the maximum antenna gain for the reader is limited to 6 dBi, resulting in a maximum total Effective Isotropic Radiated Power (EIRP) of 4W.

Readers and tags are connected to each other through a wireless channel. In that sense, we consider far-field RFID communications, in which the effective range is in the order of 10 meters [18]. Given the large number of readers that can be collocated inside a terminal (also known as Dense Reader Environment), and to avoid collisions when multiple tags are in range and try to communicate with the same reader, Medium Access Control (MAC) protocols are defined. The most used protocol in RFID communication is Slotted ALOHA, a time-based protocol in which slot allocation is carried out randomly.

RFID as a Concept for Tracking in Airports

The idea of IoT usually entails the management and processing of large amounts of data. Many Big Data applications rely on broad wireless sensor networks to provide useful information. In our case, the proposed concept addresses the passengers as the sensor network while a central processing unit gathers the information and processes it so feedback on passenger mobility and airport security can be obtained.

To that end, RFID readers are placed through an airport terminal while passengers are given an RFID tag, which enables their tracking. As passengers move, the readers identify the tags continuously and send the information to a central database where data is processed to understand the state of the terminal. Then, this data is provided to both passengers and TSA to improve mobility and security.

We identify other devices, such as mobile phones, on which the proposed system could also rely. However, although coverage may extend, exclusively depending on these connections provides a "tracking switch" to all passengers, thus opening the door to a performance decrease due to the manual deactivation – because of various reasons – of part of the sensors. In contrast, RFID tags will always transmit as long as they are reached by a reader.

Introduction to the Model

The crowded environment at an airport as well as the high reader density of the system entail an extensive space of possible architectures. Given the laboriousness of analyzing and synthesizing all potential architectures, we define the plausible architectures as a set of separated architectural decisions [19].

These decisions respond to different questions that need to be answered before the implementation of the system in a real terminal: Which passengers should it track? Where does the system start and finish the tracking? Which specific RFID technology shall we consider? Is it necessary to fix particular protocols? How many readers should we place? How should we distribute them?

To be able to optimize the architecture with the best option for each of the decisions, in the following sections we develop a simulation model combining all the elements of the RFID system, as well as the terminal in which it operates and the passengers that have to be tracked. To support the model disclosure, Figure 1 shows its diagram with the different subparts and how these interact with each other.

3. AIRPORT MODEL

The first step in the development of the model is the creation of the system's context – the part that all architectures share – which is the airport terminal itself. This means simulating not only the physical space of the terminal but also the passengers and their trajectories through it.

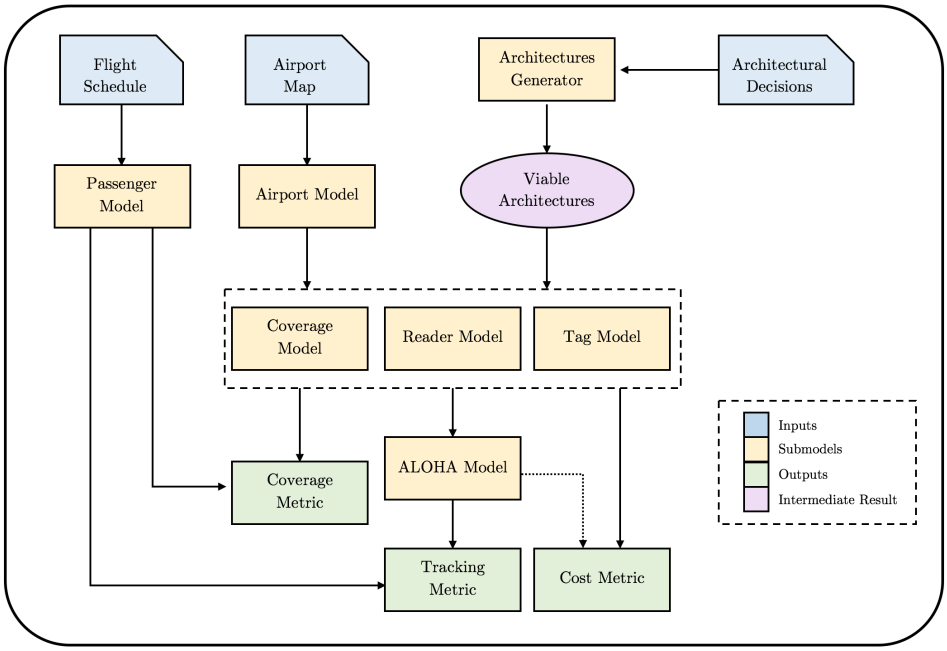

Figure 1. **Diagram of the model.**

Terminal

Terminal simulators have already been described in literature with the aim of providing insightful information for facility design [20] or optimizing passenger flow [21]. In our case, we want to simulate the airport and then simulate an RFID communication system on top of it, thus differing from airport simulators' usual goals.

To begin with, we focus just on airport passenger buildings, as neither plane runways nor other locations such as the car rental area will be populated with RFID readers. A passenger building is a 3D environment but passengers walk across 2D planes; therefore we model the buildings as flat surfaces, following the same concept of other airport simulators [22].

Motivated by the amount of data available from the airport, we choose to model the Terminal 3 at Chicago O'Hare International Airport (ORD). Four of the nine concourses the airport are located in Terminal 3, which hosts domestic flights from several well-known airlines. Figure 2 shows the map of the chosen building.

Figure 2. **Map of the Terminal 3 at Chicago O'Hare International Airport.**

To model the layout of the terminal as a flat surface we regard the map as a discrete domain consisting of tiles, and assign each of these tiles a different number depending on whether they are walking areas, obstacles or outer regions. Therefore, we define the terminal T as

$$T = (t_{ij}) \in \mathbb{R}^{m \times n} \tag{1}$$

We set m and n to be 1200 and 1450, respectively. This way, each tile has a real size of 0.38 meters, half the human average stride length [23]. With this value we achieve the necessary granularity to differentiate the RFID coverage of the different architectures.

Next, we define a *location* as a site at the airport that is part of a passengers' trajectory and belongs to a certain class, such as entrances, check-in counters, security points or gates. Then, a single location l_k is defined as the tuple

$$l_k = (i_k\,,\, j_k\,,\, c_k)\,, \tag{2}$$

where i_k and j_k are the coordinates of the location's tile in T and c_k is its class. A location occupies exactly one tile. In Figure 3, the Terminal 3 of O'Hare airport is presented following the modeling described in this section. Black areas correspond to the outer regions of the terminal, white areas represent walking areas, and finally gray areas model obstacles in the terminal. These obstacles may be closed spaces, such as shops or restaurants, or restricted walking areas, such as security control points.

Colored dots in Figure 3 represent the position of each loca-

Figure 3. Model of the Terminal 3 at Chicago O'Hare International Airport.

tion l_k. Thirteen red dots represent the different entrances; check-in counters are showed as twenty-eight blue dots; ten green dots indicate various security control points; seventy-eight yellow dots represent the gates of the terminal; and finally a single purple dot models the exit of the terminal for arriving passengers, which leads them to the baggage claim area and exit.

Passengers

Modeling of human walking has already been studied for numerous purposes and applications [24][25][26]. However, current walking models present such a high level of detail and complexity that using them to create more than 100,000 passengers who are walking distances over 300 meters would take an excessive amount of time and computing resources. To alleviate this constraint, we create a simpler long-distance walking heuristic able to handle scalability issues.

As in [27], we model trajectories as a succession of locations $l_1, \cdots l_K$ in the form of way points, each of which represents a way point that the passenger must go through before completing the entire journey (recall here the distinction between *location* and *tile*). For instance, departing passengers that enter the terminal for the first time may first head to the check-in counter, then walk towards the security point and finally reach the corresponding gate. Formally, we define a passenger trajectory PT_l as set of steps s_{lk}

$$PT_l = (s_{l1}, s_{l2}, \cdots, s_{lK}) \tag{3}$$

where each step s_{lk} is defined by its coordinates

$$s_{lk} = (i_{lk}\ ,\ j_{lk}) \tag{4}$$

While reaching each location, passengers are only able to walk through walking areas, and can not cross obstacles or move outside of the terminal. It is also obvious that no passenger can move to any tile that is not adjacent to his/her current tile.

Next, we present Algorithm 1 as our approach to computing a human-walking trajectory in the terminal context.

Each passenger has a set of predefined locations, which is represented by the *locations* array. For each type of location, the passenger is assigned one instance randomly. At the beginning of the trajectory, the passenger is placed at the first location in *locations* and sets his/her target on the second location of the array. While the target is not reached, the passenger will keep walking. Once he/she arrives at the target, the algorithm will provide the passenger with a new target until the final location is reached. Finally, the algorithm has a *break* statement in order to prevent the simulation from getting stuck in the creation of a single trajectory should the proposed heuristic fail.

Algorithm 1 compute_trajectory

```
1:  procedure ComputeTrajectory
2:      next_loc ← 1
3:      step ← 0
4:      target ← locations[next_loc]
5:      while not reached_final() do
6:          make_next_step(target)
7:          step ← step + 1
8:          if position == target then
9:              if next_loc + 1 < length(locations) then
10:                 next_loc ← next_loc + 1
11:                 target ← locations[next_loc]
12:         if step > threshold then
13:             break()
```

In real terminals, passengers mostly carry out non-optimal trajectories, as they may deviate to other places, such as shops, restaurants and restrooms. Therefore, we model the $make\_next\_step$ statement as a random variable that allows passengers to also take non-optimal directions. So, given the result of a random variable, a passenger can make three types of step:

- **Optimal**: The passenger makes the step that gets him/her closer to the target following the A* algorithm [28].
- **Logical**: The passenger makes a random step but, if the passenger is positioned next to an obstacle or wall, the algorithm will substantially increase the probability of walking in a direction that makes the passenger head away from that obstacle or wall, as people in airports do not tend to walk next to walls.
- **Random**: The passenger takes a complete random step in a direction with no obstacles.

Once the model chooses the direction in which a passenger has to walk, this passenger walks more than one step in that direction. Figure 4 shows an example of a trajectory created by the model.

In addition to creating the passengers in the spatial domain, it is necessary to place them in the temporal domain. To model the time passengers stay inside the terminal, we have to consider departing and arriving passengers separately. On the one hand, departing passengers usually arrive more than an hour before the flight and have to spend time waiting to board. On the other hand, arriving passengers enter the terminal the moment they walk through the boarding gate and do not stop until they reach the baggage claim area or the exit.

Unfortunately, we lack real data on the temporal behaviour of passengers and can not model this feature as accurately as we would like to. However, we can base our approach on Reference [29]. In that sense, we develop two heuristics, one for each travel direction – departure and arrival – by which we try to model how different passengers from the same flight have different arrival times. For the departing case, we define

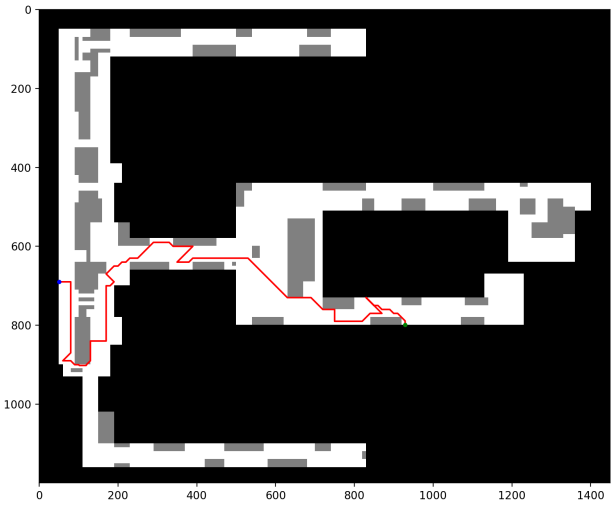

Figure 4. Example of a passenger's trajectory created by the model.

the time spent inside the terminal t_{t_d} as

$$t_{t_d} = walking\ time + t_{early} + t_{b_d}, \tag{5}$$

where t_{early} captures the time a passenger has to wait because of the early arrival at the airport and is defined as $t_{early} \sim N(2500\,\text{s},\ 500\,\text{s})$; and t_{b_d} represents the time a passenger spends waiting from the moment the boarding starts until she/he boards, modeled as $t_{b_d} \sim N(0,\ 240\,\text{s})$.

In contrast, the heuristic developed for the arriving case is much simpler. The time spent inside the terminal for the arriving passengers t_{t_a} is defined as

$$t_{t_a} = walking\ time + t_{b_a}, \tag{6}$$

where t_{b_a} represents the different times passengers disembark from the plane and therefore walk through the boarding gates. It is defined as $t_{b_a} \sim |N(0,\ 200\,\text{s})|$, given that arriving passengers spend less time queuing than departing ones, as no ticket checking is needed.

4. Communications Model

In the literature we find studies that involve the creation of RFID simulators. Two good examples are: RFIDSim [30], a physical and logical layer engine for passive RFID simulation; and the PARIS Simulation Framework [31], an RFID simulation environment that focuses on the physical layer, particularly the UHF communication channel. Unfortunately, both models are computationally intensive and would require large resources to apply directly into our airport simulation environment. Therefore, we have created a new RFID model focusing on a scaled version of current simulators in exchange of level of detail.

For the purposes of this study, the communications model has been divided into two major parts: Computing the antenna locations within the terminal, and quantifying the performance of the system vis-a-vis the MAC protocol. For the former, we first need to compute the effective range of any given reader. Therefore, we utilize the link budget equation to compute the maximum distance that can separate a tag and a reader given the reader's antenna technology its sectorization pattern. On the other hand, a model for the Slotted ALOHA protocol used in RFID systems is utilized to quantify the percentage of tags detected per reader as a function of the number of tags in a reader's vicinity.

Link Budget

Two communication links are established through the wireless channel: A downlink in which the reader transmits a modulated RF signal to the tag, and an uplink in which the tag's integrated circuit (IC) varies the input impedance and responds using a backscattering mechanism [32]. Reference [33] demonstrates that the downlink is more restrictive than the uplink as the power sensitivity threshold of the tag is lower than that of the reader.

The equation expressing the power P_{rt} received by the tag in the downlink communication can be expressed as [33]

$$P_{rt} = P_{tr} G_{tr}\, P_L\, g_{rt} \chi \tau, \tag{7}$$

where $P_{tr}G_{tr}$ is the reader transmitted EIRP, g_{rt} is the gain of the tag's receiver antenna, χ is the polarization matching coefficient, and τ is the impedance match between the antenna and the RFID chip. P_L represents path loss, which strongly depends on the propagation environment. In that sense, if we consider the *Free Space Propagation Model*, then the path loss would be expressed as [34]

$$P_L = \left(\frac{\lambda}{4\pi d}\right)^2, \tag{8}$$

where λ is the signal's wavelength, and d is the distance between the reader and the tag. As airports are enclosed spaces, we could also consider the *Indoor Large Scale Propagation Model*, in which case the equation for path loss is [34]

$$P_L(d) = P_L(d_0) + 10n \log\left(\frac{d}{d_0}\right) + X_\sigma(\text{dBW}), \tag{9}$$

where d_0 is an arbitrary reference distance, $P_L(d_0)$ is the free space path loss for distance d_0, n is the path loss exponent, and X_σ is a zero mean Gaussian random variable that models environmental factors such as tag obstruction or multipath propagation.

Equation 7 constitutes the link budget equation of the model, which allows us to compute the maximum distance between reader and tag such that the latter receives enough power to operate. To that end, we make the following assumptions:

- The received power P_{rt} has to equal the power sensitivity of the tag, $P_{rt} = S_t$.
- The power transmitted by the reader, is limited to 4W according the regulations presented in Section 2. Therefore, $P_{tr}G_{tr} = 4\,\text{W}$.
- We assume the gain of the tag's receiver antenna is equal to one, so $g_{rt} = 0$ dB.
- We assume a circular polarized reader antenna and a linearly polarized tag; then the sensitivity to polarization can be

ignored but an additional 3 dB loss has to be considered [33]. Therefore, $\chi\,(\mathrm{dB}) = -3\,\mathrm{dB}$.
- We make the assumption that there are no losses due to the impedance match, $\tau = 1$.
- We neglect the large-scale and small-scale fading modeling, as they are too complex for the scope of this paper.
- We assume the collocation of readers at admissible altitudes and therefore model 2D RFID communications.

Next, we consider the two aforementioned propagation models: The free-space wireless channel path loss, in Equation 8; and the indoor large scale propagation wireless channel model, in Equation 9, in which we set the arbitrary distance d_0 to be one meter, consider a path loss exponent $n = 2$ or $n = 3$ and neglect the Gaussian random variable, $X_\sigma = 0$. Finally, to fully specify the link budget equation, we still have to define the tag's power sensitivity S_t, which primarily depends on its IC. In that sense, we consider and compare three different models: *Higgs-3*, *Higgs-4* and *Higgs-EC*, whose sensitivity is -20 dBm, -20.5 dBm and -22.5 dBm, respectively.

In Table 1 we present the maximum reading distances obtained when applying Equation 7. In all cases the carrier frequency is set to 915 MHz.

Table 1. **Maximum reading distances for each tag IC and wireless propagation model**

Tag IC	Propagation Model		
	Free-space	**ILS,** $n = 2$	**ILS,** $n = 3$
Higgs-3	11.65 m	11.65 m	5.88 m
Higgs-4	12.35 m	12.35 m	6.11 m
Higgs-EC	15.54 m	15.54 m	7.13 m

The first two models provide same results. This is because the indoor large scale model turns into the free-space model when $n = 2$. In contrast, when using the indoor large scale model with $n = 3$ we obtain significantly lower values for the maximum operation distance. Finally, given that the values obtained with $n = 2$ are more consistent with the results in [12], we assume that the *Free Space Propagation Model* provides a sufficient approximation for the purposes of this paper.

Sectorization and Coverage

The idea of covering the terminal inevitably comes hand-in-hand with the concept of sectorization. As in cellular networks, we wish to divide the terminal in regions in which omnidirectional coverage is achieved. Although RFID omnidirectional antennas are being studied in the literature (see, for instance, [35], [36]), commercial RFID antennas mostly present a directional gain profile. Therefore, we sectorize each reader with multiple (three or four) RFID directional antennas in order to approximately obtain an omnidirectional radiation pattern. In particular, our calculations are based on the ALR-F800 reader together with the ALR-A0501 antenna [37]. This antenna, whose radiation plot is showed in Figure 5, stands out for its lower directionality as compared to other available models (note that the 3dB beamwidth of this antenna is approximately 105°).

Figure 6 and Figure 7 show the approximate radiation plots that would result from connecting three and four ALR-A0501 antennas to an ALR-F800 reader. Note that the resulting radiation patterns are not perfectly omnidirectional. Therefore, we proceed by estimating the gain loss ΔG_t in the reader's antenna that results from pointing in a non-optimal direction of the radiation pattern. In that sense, our conservative criteria selects a gain loss such that 90% of the azimuth plane sees a gain $G_t \geq G_{t,max} - \Delta G_t$.

For the three antennas case, we note that the 3 dB beamwidth of the three antenna configuration covers almost the 90% of the azimuth plane, so we consider the range of the omnidirectional coverage as the maximum range with an extra 3 dB penalization. On the other hand, for the four antennas case, approximately the 90% of the azimuth plane is covered by the 1.5 dB beamwidth. So, we penalize the link budget equation with an extra 1.5 dB loss, as it is the difference between the maximum gain of the antenna and the gain at $45\,\mathrm{deg}$.

In Table 2 we show the resulting coverage ranges for each of the previously mentioned ICs depending on the number of antennas connected to the same reader. We observe that, in general, connecting four instead of three antennas results in a range improvement of approximately 1.5 to 2 meters.

Table 2. **Coverage ranges for each tag IC given a number of connected antennas**

Tag IC	Number of antennas	
	Three (3 dB loss)	**Four (1.5 dB loss)**
Higgs-3	8.25 m	9.81 m
Higgs-4	8.74 m	10.39 m
Higgs-EC	11.00 m	13.08 m

Reader Placement and Channel Allocation

Once we have quantified the range of coverage for a single reader, we are now ready to discuss the placement of the readers within the terminal. For instance, in Figure 8 we present an illustrative example of reader placement where the radius of each circle is equal to the maximum coverage range, and its color represents the UHF channel used for communicating with the tags. Note that both the placement of the readers and the channel assignments are, in this figure, completely random, but will need to be optimized in our model.

The antenna placement and channel allocation problem can be summarized as follows: Given a fixed number of readers with a pre-specified range, a fixed number of channels within the UHF band, and a certain area to cover within a terminal, we seek to maximize the percentage of area covered by at least one while minimizing the number of necessary readers and avoiding intra or interchannel interference. This problem is a clear example of the Antenna Placement Problem (APP), a subtype of "covering problem" [38] which has already been addressed for the RFID case [39]. In other words, the APP poses the question of how many and where we should place different base stations given a set of candidate points and a set of constraints.

The most common solution to the problem is based on genetic algorithms, a type of optimization algorithm inspired by natural selection [40]. The application of genetic algorithms to solve the APP has already been studied in literature [41]. Unfortunately, when the number of candidate points increases, genetic algorithms require increasing amounts of time to converge to the optimal solution. In our case, where we have more than a thousand candidate points, and more

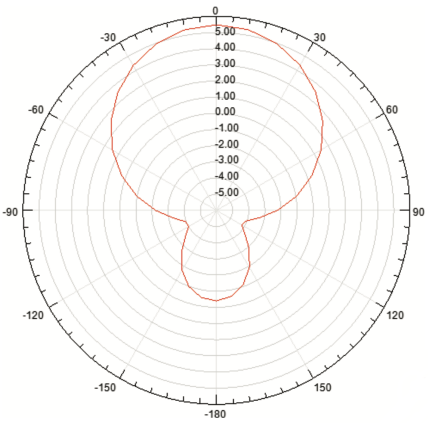

Figure 5. ALR-A0501 antenna radiation plot.

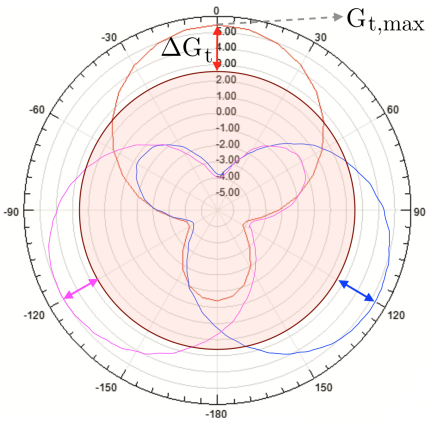

Figure 6. Three ALR-A0501 antennas radiation plot.

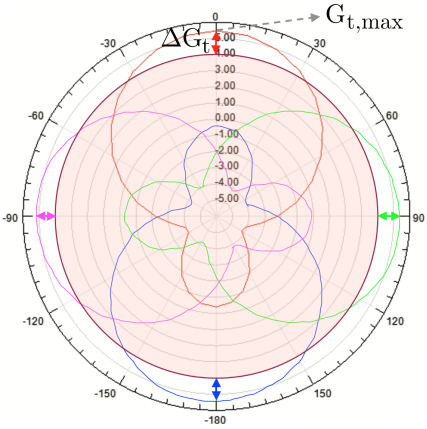

Figure 7. Four ALR-A0501 antennas radiation plot.

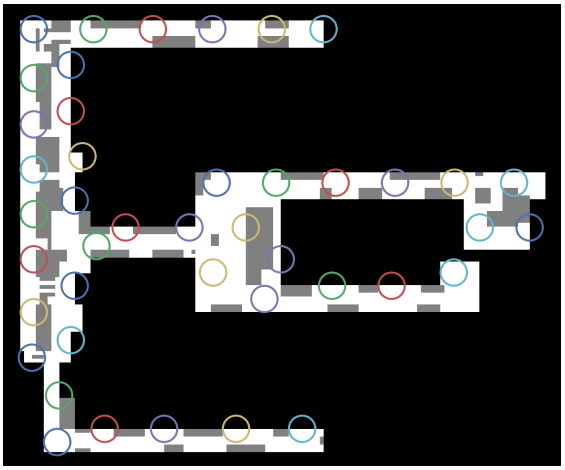

Figure 8. Illustrative example of a simple placement of RFID readers within the modeled terminal.

than a hundred architectures, each with its own APP, the use of genetic algorithms is not possible due to excessive computational burden. Instead, we develop a suboptimal heuristic placement algorithm shared across all architectures that satisfies the channel interference restrictions while being computationally inexpensive.

To develop this heuristic, we start by considering Reference [17], where a study on the minimum distances between RFID readers to avoid interference is presented. Table 3 shows the results of this study and considers both the relative position of antenna pairs and their degree of channel adjacency (e.g. if channel adjanceny is zero, then both readers are using the exact same frequencies to transmit). Although these distances may vary with the technology, we can notionally see how far apart two readers with the same channel allocation need to be assuming a directional antenna.

Instead of introducing these distances as restrictions in our heuristic, our heuristic algorithm tries to cover the terminal, given the range of a reader and a separation parameter, while minimizing the amount of overlap between reader coverage areas. The algorithm works as follows:

1. The algorithm is given the coverage radius and the horizontal separation between readers as inputs.
2. It iterates through all the tiles of T, from left to right and from top to bottom.
3. If a tile $t_{i,j}$ is empty, it places a reader there and moves to tile $t_{i,j+separation}$ to continue with the placement.
4. When the algorithm reaches the end of row i, if it has placed any reader in that row, jumps to row $i + radius$, $i + 1$ otherwise.
5. The algorithm finishes as soon as it reaches the bottom-left corner of the terminal.

Table 3. Safe distance for different antenna configurations [17]

Channel Adjacency	Antenna of Default Configuration		
	Front (m)	Side (m)	Back (m)
0	1400	350	210
1	180	45	30
2	130	25	15
3	95	20	10

Once the placement for all readers within the airport terminal has been obtained, we proceed to allocate UHF channels to each of them. In that sense, we use Algorithm 2 as a heuristic approach to assign non-adjacent channels to contiguous readers such that the channel interference is minimized. Note that Algorithm 2 can be interpreted as a Depth-First-Search (DFS) through the tree of all possible channel assignments given the readers and its locations.

Algorithm 2 Obtain Channel Allocation

```
procedure ITERATE_READERS(r_array, i)
    if i == length(r_array) then
        return True
    else
        for c ∈ [1, 50] do
            if check_channels(r_array, i, c) then
                r_array[i].channel ← c
                if iterate_readers(r_array, i + 1) then
                    return True
                r_array[i].channel ← −1
        return False
```

At each step of Algorithm 2, we iterate over all readers in the terminal, allocate a new channel to one of them and then check the viability of the resulting allocation. If a new reader can not communicate through any channel without causing interference, the algorithm changes the channel allocation of the previous readers, until it reaches convergence. To check the viability of the placement at each step we develop Algorithm 3.

Algorithm 3 Check Channel Interference

```
1:  procedure CHECK_CHANNELS(r_array, i, c)
2:      for r ∈ r_array[: i − 1] do
3:          if check_line_of_sight (r_array[i], r) then
4:              dist ← get_distance (r_array[i], r)
5:              channel_diff ← abs (c − r.channel)
6:              if channel_diff == 0 & dist ≤ 1400 then
7:                  return False
8:              if channel_diff == 1 & dist ≤ 180 then
9:                  return False
10:             if channel_diff == 2 & dist ≤ 130 then
11:                 return False
12:             if channel_diff == 3 & dist ≤ 95 then
13:                 returnn False
14:     return True
```

The algorithm focuses on reader i and iterates over all the other readers which a channel has been already assigned to each. First, it checks whether reader i has direct line of sight (LOS) with each of the other readers. We not only consider as LOS a clear path between readers but we also, trying to be conservative, allow an obstacle as thick as 8 meters. So, if a reader is in LOS with reader i, we compute the distance between readers and the distance between the readers' assigned channels. We then compare both measures with the interference-safe values from Table 3, assuming both readers have face-to-face antennas and therefore considering the most restricted case, being the Front Configuration.

To obtain the minimum distance we evaluate different separations in terms of the coverage radius. We find this minimum distance corresponds to 2.5 times the radius. This does not mean we must choose this value but that no distance we select can be smaller than 2.5 times the radius.

Medium Access Channel Protocol

As mentioned in Section 2, Slotted ALOHA is the most used protocol in RFID systems and therefore we choose it for the simulation of our system. The protocol works as follows:

- There is a reader and a set of n unidentified tags.
- The reader starts the communication process by providing N time slots and starting an identification cycle that broadcasts to all tags in range.
- The tags receive the number of slots N and randomly select one to communicate their IDs back to the reader.
- The reader receives some slots empty, others with one tag's ID, and the rest are corrupted due to data collisions from two or more tags.
- The reader triggers more cycles until it completes the full set of cycles. Once a tag is identified for the first time, it will remain identified during the following cycles for the rest of the set of cycles.
- Once the reader finishes with the identification process, all tags go unidentified again and the reader has to restart the complete set of cycles.

Several Slotted ALOHA protocols applicable to RFID systems have been presented in the literature. One of the simplest algorithms is the Basic Framed Slotted ALOHA (BFSA) algorithm, which although easy to implement, causes inefficiencies when selecting optimal slot frame sizes [42]. In [43], the Dynamic Framed Slotted ALOHA (DFSA) is presented, and its Advanced (AFSA) version is introduced too. Both algorithms try to estimate the number of tags present in the area before deciding the frame size. Finally, in [42] the Enhanced Dynamic Framed Slotted ALOHA (EDFSA) is presented and is shown to notably outperform BFSA in terms of frame size efficiency. When the number of tags exceeds 500, we can also appreciate how EDFSA provides a more slot-efficient approach than DFSA. Given the scope of our problem, where it is unlikely to have more than 500 tags per reader, we select the DFSA/AFSA algorithm as the baseline protocol for the MAC functionality.

Following the work in [43], we start by introducing some mathematical preliminaries. Given a reader R, which provides N slots to the set of n tags that it covers, the number r of tags in one slot —called occupancy number— follows a binomial distribution with parameters n and $\frac{1}{N}$:

$$B_{n,\frac{1}{N}}(r) = \binom{n}{r}\left(\frac{1}{N}\right)^r\left(1-\frac{1}{N}\right)^{n-r} \tag{10}$$

Applying Equation 10 to all N slots, the expected value of the number of slots with occupancy number r is given by $a_r^{N,n}$ [43]:

$$a_r^{N,n} = N\,B_{n,\frac{1}{N}}(r) = N\binom{n}{r}\left(\frac{1}{N}\right)^r\left(1-\frac{1}{N}\right)^{n-r} \tag{11}$$

DFSA algorithm estimates the number of tags present in the reader's radius before selecting an optimal frame size. To that end, the reader first provides a frame size of N slots. The received frame, resulting from a tag-reading cycle, can be viewed as the tuple $\langle c_0, c_1, c_k\rangle$, in which each number quantifies the number of empty slots, slots filled with exactly one tag and slots with collisions.

Given these three numbers we can estimate a lower bound for the number of tags n [43]:

$$\varepsilon_{lb}(N, c_0, c_1, c_k) = c_1 + 2c_k \tag{12}$$

This expression meets the requirement that there can not be less tags than the number of slots filled with one tag plus two times the number of slots in which a collision has taken place. A collision requires a minimum of two tags filling the same slot in order to occur, that is why c_k is multiplied by two.

Once the reader knows a lower bound for the number of tags n, it can compute a more accurate estimation [43]:

$$\varepsilon_{vd}(N, c_0, c_1, c_k) = \min_n \left| \begin{pmatrix} a_0^{N,n} \\ a_1^{N,n} \\ a_{\geq 2}^{N,n} \end{pmatrix} - \begin{pmatrix} c_0 \\ c_1 \\ c_k \end{pmatrix} \right| \tag{13}$$

The reader looks for the value for n that minimizes the error between the expected numbers of slots filled with zero, one or two or more tags, given by Equation 11, and the actual quantities observed in each case. We update the size of the slot frame accordingly to $N = \lfloor n \cdot e \rfloor + 1$. The reason of this number is that given a number of agents k following a Slotted ALOHA MAC protocol, the frame size that provides the optimal throughput is $N = k \cdot e$ [44].

Once the slot frame size is fixed, all tags in range select a random slot to communicate again. Then, the reader checks the total number of tags that have filled each slot and, among those slots that are filled with just one tag, looks for that tag's ID to check if it is already within the detected group. If not, these tags are then added to the detected group. Note that it is possible, in some cases, to have tags not detected at the end of set of identification cycles. In other words, even if a passenger is within range of a reader, it is possible that she/he is not properly identified and tracked.

We have previously explained that, for a correct detection of all tags in range in a relatively short amount of time, RFID readers perform a set of identification cycles. The more cycles performed, the higher the chances of a 100% identification. However, since the impact of having extra cycles minimally reflects on the cost of the energy consumed, we decide to use a time-limited approach for our model. Hence, we set a 5 seconds limit to a set of cycles, so a reader can perform as many cycles as needed inside that 5 second frame. We choose this value because, considering the average adult human walking speed lies around 1.5 m/s [45][46], we ensure every passenger crossing a coverage area close to its center will be detected and possibly identified at least once.

5. ANALYSIS

Architectural Decisions

In Table 4 we present the summary of the decisions considered for the model and the architectural tradespace in the form of a Morphological Matrix. Since the number of architectures in this case is relatively small, we follow a Full-Factorial Enumeration strategy and simulate each of the 144 architectures. Next, we proceed by analyzing each of them and their impact in the overall system architecture.

We have already mentioned different types of passengers can travel in different directions inside a terminal. In particular, we consider two primary types: Passengers departing and passengers arriving. Therefore, the two first major decisions select whether each of these passengers will be tracked or not.

- **Decision 1**: *Do we track departing passengers?*
- **Decision 2**: *Do we track arriving passengers?*

Furthermore, there is a third type of passengers, those who connect from one flight to another one. Due to the absence of real data on connecting passengers, we opt for not simulating them in this work. Still, we bear the *Tracking Connecting Passengers* decision in mind.

Although the three types of passengers are in the same terminal, they follow different trajectories and move through different areas. Therefore, it is important to specify where should we place the readers inside the terminal in order to cover all possible trajectories effectively. To achieve that, we create two architectural decisions that select the initial and final tracking point for departing passengers. Note that the same two decisions could also be specified for arriving passengers. However, their trajectories go directly from the gates area to the terminal exit and, consequently, these decisions would be equivalent to deciding whether to track or not track arriving passengers (i.e. Decision 2).

- **Decision 3**: *Which is the initial tracking point for departing passengers?*
- **Decision 4**: *Which is the final tracking point for departing passengers?*

Once we have determined the limits of the tracking area, we have to decide how we should place the readers inside that area. We have previously introduced a heuristic to place readers and specified the minimum horizontal distance between readers. However, we have not agreed on using 2.50 the radius as the definitive distance between readers. That is why we turn the distance into a decision:

- **Decision 5**: *Which is the horizontal distance between readers?*

To be able to see the impact of this decision on the tradespace, apart from choosing the minimum distance, we also consider 2.75, 3, and 3.25 times the radius as options for the horizontal separation between readers.

During the development of the model we also focused on RFID antennas. Specifically, we considered the use of more than one antenna and showed two possible configurations using 3 and 4 antennas, respectively. Therefore:

- **Decision 6**: *How many antennas should we connect to readers?*

Regarding RFID tags, in this paper we have compared three different models of tags' integrated circuits – *Higgs-3, Higgs-4*, and *Higgs-EC* – during the development of the RFID model in Section 4. From Table 1 and Table 2 we can observe that *Higgs-EC* outperforms the other ICs. Consequently, one could think that *Higgs-EC* is also more expensive than the others. However, after speaking with a sales responsible from an RFID supplier company, we learned *Higgs-EC* was actually the cheapest. This is due to the reduced manufacturing costs as well as the eagerness of the industry in adopting new and better tag models. Consequently, we assume that *Higgs-EC* dominates the other IC options both in performance and cost and therefore we select it for our analysis.

Metrics

To compare the different architectures and be able to discern which of them provides the best results, it is necessary to select some evaluation criteria. Ideally, we would like to point out which architecture is the one that provides the greatest value, defined as benefit at cost. In order to measure the benefit and the cost separately we create both a performance metric and a cost metric, and assign each architecture two individual values that allow placing that architecture in an architectural tradespace [47].

Cost Metric—For the cost metric, we first consider all costs involved in the system and use normalized US Dollars as the cost unit. We divide the costs involved in the architectures in the following three categories:

- **Technology Cost**: Readers, Antennas and Tags.
- **Installation Cost**: Human Labour and Cabling.
- **Operation Cost**: Human Labour and Energy.

Table 4. Morphological Matrix containing all the decisions considered for the system's model

Architectural Decision	Option 1	Option 2	Option 3	Option 4
Tracking Departing Passengers (TDP)	Yes	No		
Tracking Arriving Passengers (TAP)	Yes	No		
Departing Initial Tracking Point (DITP)	Entrance	Check-in Counter	Security Point	None
Departing Final Tracking Point (DFTP)	Check-in Counter	Security Point	Gate	None
Horizontal Distance Between Readers (HDBR)	2.50 radius	2.75 radius	3.00 radius	3.25 radius
Antennas per Reader (APR)	3	4		

Of these, we choose to take into account only the cost of readers and antennas. The rationale for this choice is twofold: First, other costs such as human labour are approximately fixed across all architectures and therefore would not have an impact in the relating costing metric of the tradespace. Second, energy costs and cabling costs are at least one order of magnitude lower than the other costs, thus allowing us to neglect them in this study. Finally, the cost metric utilized in the results is

$$C_{total} \approx C_{technology} \approx C_{readers} + C_{antennas}. \tag{14}$$

Performance Metrics—Two performance metrics are considered in this analysis. The first one measures how well the terminal is covered by readers given communication range constraints and channel allocations constraints. In contrast, the second one quantifies how well passengers covered by at least one reader are tracked given the S-ALOHA identification protocol.

In Section 3 we defined a passenger's trajectory as $PT_l = (s_{l1}, s_{l2}, \cdots, s_{lK})$, where each s_{lk} corresponds to a step of the trajectory that has coordinates i_{lk}, j_{lk} associated with it. Given a trajectory PT_l, we now define its coverage C_l as

$$C_l = (C_{l1}, C_{l2}, \cdots, C_{lK}) \tag{15}$$

where each C_{lk} is either 1, if the step s_{lk} is covered by a reader, or 0, if it is not. So, as the main performance metric, we define the percentage of spatially covered trajectory P_C as

$$P_C = \frac{1}{N_P} \sum_{l=1}^{N_P} \frac{1}{N_{lK}} \sum_{k=1}^{N_{lK}} C_{lk}, \tag{16}$$

where N_P is the total number of passengers that get in the terminal during the whole simulation time frame. We define it as "spatial" because we consider the amount of a passenger's path that is covered and not the amount of time a passenger is being covered (temporal coverage).

During its trajectory, each passenger tag will need to be identified several times. We define these requests R_l as

$$R_l = (r_{l1}, r_{l2}, \cdots, r_{lQ}), \tag{17}$$

where r_{lq} is either 1 if the tag is correctly identified in time q, or 0 if it is not. Then, the second performance metric P_T, dealing with the tracking, is defined as follows

$$P_T = \frac{1}{N_P} \sum_{l=1}^{N_P} \frac{1}{N_{lQ}} \sum_{q=1}^{N_{lQ}} r_{lq} \tag{18}$$

Results

Since we are interested in modeling a real day of activity at Chicago's airport, we extract real data from the Chicago O'Hare Airport's flights schedule website. This data contains not only the plane's arrival or departure times, but also the boarding gates of each of these flights. As a baseline case, we model the complete flight schedule of Thursday, July 27$^{\text{th}}$ 2017. That day, a total of 1,122 flights were scheduled, divided in 572 departures and 550 arrivals.

Next, in Figure 9 we present the architectural tradespace as well as the Pareto Front. All architectures show both the coverage metric in the x-axis and the cost metric in the y-axis.

At first glance, there exists a proportional relationship between the performance and the cost of this system. So, if a coverage of more than a 70% is to be achieved, the cost of the system inevitably rises to more than 75% of the maximum cost. Then, the Pareto Front is composed by 14 architectures – 9.7% of the total – that span from low-cost-low-performance systems to high-cost-high-performance alternatives. Starting from the low-cost region, the Pareto Front presents a tendency such that an increase in performance comes alongside an increase in the cost of the architecture. Then, it changes and we enter a stage in which we can achieve substantial increases in performance with minimal increases in cost. Finally, the Pareto Front goes back to the initial tendency until it reaches the high-cost-high-performance area. From this, we can see how easily we can move across the range of 30%-50% in performance without noticing a significant change in cost.

Departing Initial Tracking Point— After introducing the Pareto Front, we focus on determining how each of the architectural decisions affects the tradespace. In the same Figure 9

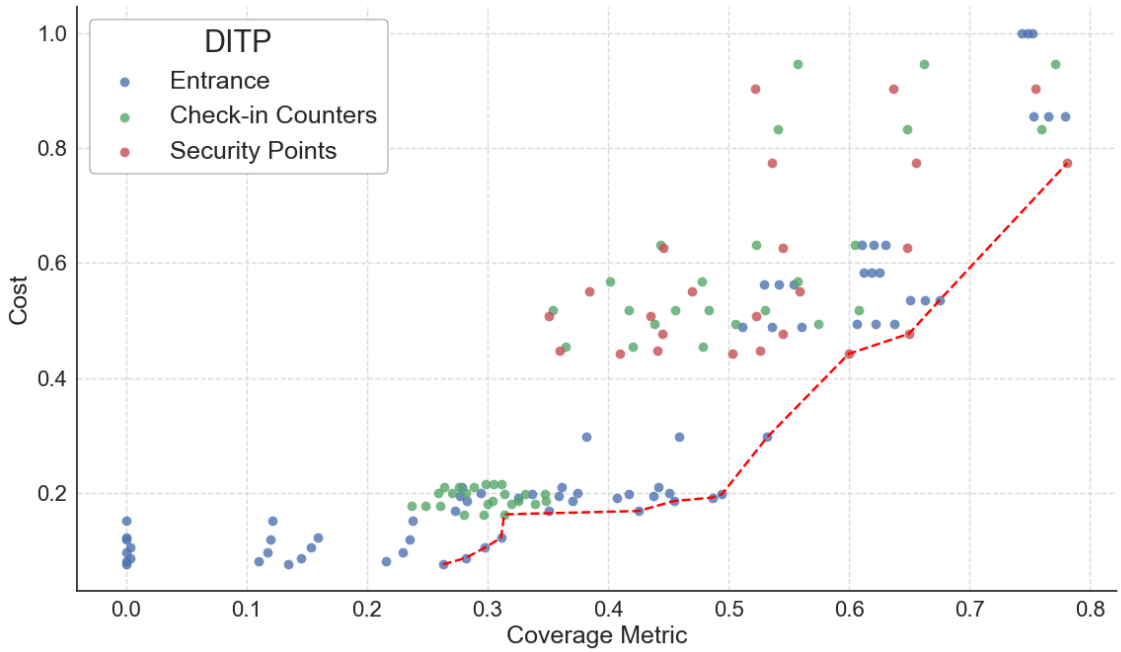

Figure 9. Architectural Tradespace, Pareto Front and Impact of the Departing Initial Tracking Point decision on the Architectural Tradespace for the baseline case.

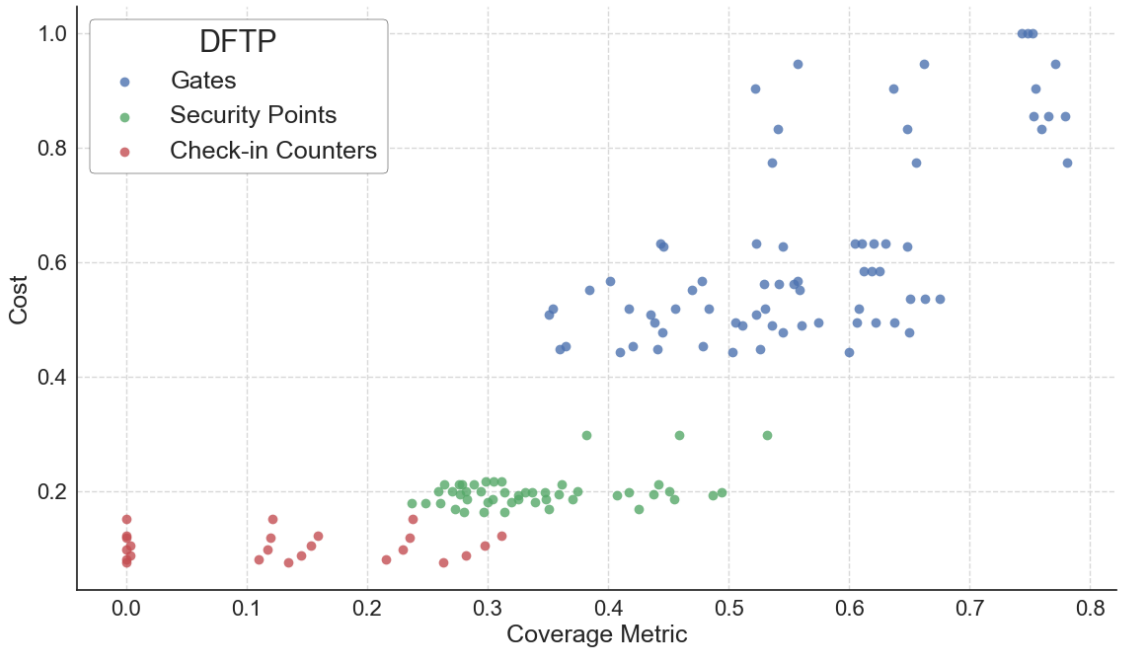

Figure 10. Impact of the Departing Final Tracking Point decision for the baseline case.

the effect of the *Departing Initial Tracking Point* decision is showed. Although most of the non-dominated architectures present the entrance of the terminal as the initial tracking point, this must not be confused with dominance; as in the low-cost-low-performance region there is no other possible option than starting at the entrance, as observed in Figure 10. In the high-cost-high-performance region, where there is presence of the three options for the DITP decision, these architectures are sometimes dominated by the architectures tracking from the security point to the gates. However, from the medium-cost-medium-performance region we can clearly conclude the architectures with DITP = "Entrance" dominate the architectures with DITP = "Check-in Counters".

Departing Final Tracking Point—In Figure 10, we can appreciate that the DFTP decision marks the cost limits of the system, which is closely related to the number of readers needed. In the O'Hare airport, most of the surface is comprised between the security points and the gates. Therefore, if readers are placed on that area – DFTP set to "Gates" option – the amount of coverage substantially increases as well as the number of readers needed to cover the surface according to the heuristic used. In contrast, if readers are limited to the area between the entrance and the check-in counters, the maximum amount of possible surface to be covered is notably small – 30% – resulting in the reduced cost of these architectures.

Horizontal Distance Between Readers—There is a cost gap between architectures that have the same option for the DFTP decision in the high-cost-high-performance region. This gap is explained by the *Horizontal Distance Between Readers* decision. The 24 architectures on top of the gap, or high-cost region, present 2.50 times the radius as the option for the HDBR decision. When the distance between readers is reduced, more readers can be fit in the same space, hence increasing the coverage and the cost. Then, the architectures comprised between the 40% and 65% of the maximum cost show the rest of the options – 2.75, 3.00 and 3.25 times the radius – for the HDBR decision, without any of these options standing out as the dominating option.

Antennas per Reader—Regarding the APR decision, the results show that all of the architectures in the Pareto Front but one display the 4 antennas option for this decision, indicating there is a clear advantage in using 4 antennas instead of 3. We can understand the nature of the result considering the fact that the 4 antennas configuration only represents an increase of 8% in cost while the increase in coverage area elevates to 40%.

Interaction between TDP and TAP—If we look back to Figure 9 we can appreciate there are trios of architectures that have the same cost but different performances. This difference lies in the chosen options for the *Tracking Departing Passengers* and *Tracking Arriving Passengers* decisions. Specifically, these decisions show their effect in the form of an interaction, as shown in Figure 11. The difference in performance for the architectures that only differ in the TDP and TAP decisions is not constant, nor the TDP-TAP configuration that presents the best performance. On the one hand, in the low-cost-low-performance area, the readers are placed in the zones where only departing passengers go through. Therefore, when only arriving passengers are tracked, we obtain a set of architectures with zero performance; whereas focusing only on departing passenger provides the best results. On the other hand, in the high-cost-high-performance region, due to the fact that arriving passengers' trajectories are shorter and more straight-forward, it is easier to cover a larger portion of these passengers' trajectories than the departing passengers' ones, which are more irregular and comprise more surface, thus comprising more blind spots too.

Figure 9 shows that for high-cost-high-performance architectures which start the tracking at the entrance of the terminal, the performance gap of the TDP-TAP trios is much smaller than the same TDP-TAP separation for the other DITP options. This result reveals that starting tracking at the entrance of the airport has a more robust performance against the TDP and TAP decisions and their interaction in the high-cost-high-performance region.

At this point, we have observed the different impact each of the architectural decisions has on the tradespace. Some of the decisions have a clear advantageous option, others show their effects in the tradespace as a form of interaction and finally the rest can not be related with dominance, as they present all of their options in the Pareto Front.

Tracking Metric—We have previously developed two different metrics: The coverage metric, measuring how well a determined architecture covers the terminal; and the tracking metric, which deals with the quality of the tracking independently of the first metric. In Table 5 we present the value for the tracking metric for the architectures in the Pareto Front. Given the computational expenses of the S-ALOHA simulation, we limit the analysis to the non-dominated architectures and take as input just the 35% of the flight schedule of the baseline case.

Table 5. Metric values of the non-dominated architectures for the baseline case

Number	Metrics		
	Coverage	Tracking	Cost
1	0.781	0.995	0.774
2	0.675	0.789	0.535
3	0.650	0.990	0.477
4	0.600	0.991	0.442
5	0.532	0.811	0.297
6	0.494	0.827	0.198
7	0.486	0.839	0.192
8	0.455	0.840	0.186
9	0.425	0.844	0.169
10	0.314	0.991	0.163
11	0.311	0.850	0.122
12	0.297	0.854	0.105
13	0.282	0.858	0.087
14	0.263	0.862	0.076

There are two clearly different architecture tendencies regarding the tracking metric. On the one hand, four architectures present a tracking performance close to 100%. This four architectures are the ones in which only the arriving passengers are tracked. On the other hand, all the architectures that just track the departing passengers – there was no architecture tracking both types of passengers in the Pareto Front in Figure 9 – show a smaller value for the tracking metric. What is relevant about these architectures is the relationship of inverse proportionality between the cost and performance,

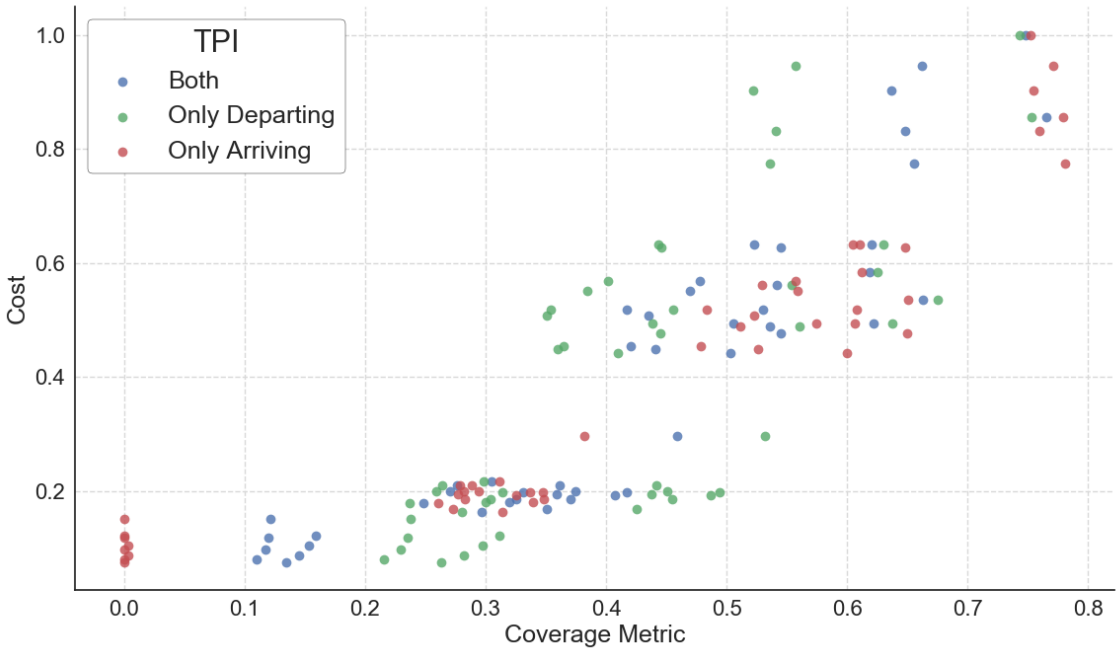

Figure 11. Impact of the interaction between Tracking Departing Passengers and Tracking Arriving Passengers decisions on the Architectural Tradespace for the baseline case.

where the best architectures in performance are the cheapest ones. The reason behind this non-intuitive result is that a decrease in the cost turns into a decrease in the number of readers, and therefore a decrease in the covered area and passengers covered simultaneously. Given we have opted for a time-limited approach regarding the ALOHA protocol, having less passengers covered makes the modeled algorithm estimate a reduced number of tags, which allows the reader to fit extra reading cycles in the 5 second time frame and therefore increase the number of detected tags.

Summary of Recommendations

In Table 6 we summarize the primary recommendation for each architectural decision. To begin the discussion, we focus on the *Departing Initial Tracking Point*. In Figure 9, we have seen how choosing to start tracking from the entrance of the terminal reduces the gaps in performance that the interaction of TDP and TAP creates. However, this only holds if the *Departing Final Tracking Point* decision is set to the "Gates" option. Finally, we note in Figure 9 that most architectures in the Pareto Front start tracking passengers from either the entrance or security points. Selecting one or the other depends primarily on the type of system under consideration, with the latter option being preferred for high performance, high cost systems.

The DFTP decision has been shown to have a major impact in the system tradespace. In fact, in Figure 10 we can observe that architectures are clearly clustered based on its value. Given that the vast majority of passengers spend most of their time in the area between the security point and the gates – in fact, the arriving passengers just walk through that area – we opt for recommending to track until the gates.

The impact of the *Horizontal Distance Between Readers* decision on the tradespace shows no preference for any of the considered options. In the high-cost-high-performance region no option clearly dominates the others, therefore we suggest a decision-making process based on further constraints such as budget or spacing limitations.

In contrast, the *Antennas per Reader* decision has a clearly preferred option. Indeed, we have shown that using 4 antennas on each reader clearly outperforms the 3 antenna configuration. This tells us that that marginal increase in cost by adding the 4th antenna is worth it given the extra performance in reader range, which in turn is used to reduce the number of readers across the terminal. Note that these conclusions are robust to tag technology, which has been shown to be a straightforward decision since *Higgs-EC* tags outperform the other alternatives in both performance and cost.

Finally, the analysis of the *Tracking Departing Passengers*, *Tracking Arriving Passengers* has been combined in Figure 11. In this case, the results of the analysis are somewhat inconclusive and do not affect the system performance and cost significantly. Therefore, we consider these decisions as secondary to the previous one, i.e. airport managers should first consider where they want to place the readers and which technologies to utilize, and then, focus on which set of passengers will be tracked.

6. CONCLUSIONS

Summary

This paper has explored the optimization of an IoAT system to track passengers within an airport terminal using RFID technology. We have initiated the work with a brief description of the goal of the system and a short literature review. Then, in Section 2 we have introduced the main features of RFID technology and presented the simulation model developed for this study.

Table 6. Recommendations for each of the architectural decisions considered during the development of this study

Architectural Decision	Recommendation
Departing Initial Tracking Point (DITP)	Track passengers from the entrance or security gates.
Departing Final Tracking Point (DFTP)	Clusters architectures in tradespace. For high performance systems, track until gates.
Horizontal Distance Between Readers (HDBR)	Second order decision
Antennas per Reader (APR)	Using 4 antennas on each reader
Tag Technology	The *Higgs-EC* IC dominates the rest of available ICs
Tracking Departing Passengers (TDP)	Approximately independent from other decisions. They can be modified after the system is implemented without major performance penalties
Tracking Arriving Passengers (TAP)	
Tracking Connecting Passengers	

In Section 3 and Section 4, we have focused on the model created to evaluate each feasible architecture. The model presents a common part that all architectures share, i.e the airport terminal and the passengers that walk across it. Second, we have showed how the RFID communications have been modeled and how each architecture differs with the others based on its option for each decision. To that end, we have presented the link budget and coverage calculations, as well as the reader placement and the communication protocol submodels.

We have started Section 5 with the discussion on the architectural decisions that define each of the possible architectures and encoded them in the form of a morphological matrix. Then, we have computed the metrics for each architecture in a baseline case and displayed the architectural tradespace, i.e. a plot that explicitely visualizes the the trade between performance and cost. After that, we have focused on each of the decisions separately in order to analyze its impact on the tradespace and its optimal architectures.

The main performance metric during the analyses has been the coverage metric. In that sense, it has been shown that the best architectures achieve a coverage score of 78% for the baseline case. This value proves that it is possible to cover most passengers in the terminal, albeit exact (and possibly optimal) placement of readers would require actual data on passenger's movement inside the Chicago airport.

We have also considered a second performance metric, the tracking metric, with which we have shown that the architectures in the Pareto Front allow the tracking function with errors in the range of 14%-20% for the architectures that just track departing passengers and errors below the 2% for the architectures that just track the arriving passengers. This tests have been performed assuming a 5 seconds ALOHA cycle duration, a sensible number given the speed at which passengers walk through a terminal. Note, however, that this value was not optimized and can therefore be refined to improve the performance of the ALOHA protocol.

Future Work

Several simplifications were assumed in this paper. Tag orientation and tag occlusion are examples of phenomena that can notably affect the performance of the system during real operations. These may be avoided by enforcing tag management policies that ensure they are not concealed at any time. Furthermore, these policies should also contemplate tag recycling inside the airport to determine when tags are first provided and possibly taken away from passengers. Such considerations can reduce the amount of tags required in the system as each one has an approximate life cycle of more than six months.

In addition, three main lines of research arise from this study. First, there is space to improve certain parts of the model used that would provide more detail to the simulation results. In that sense, models such as the reader placement model or the passengers' walking model should be refined and enhanced. Also, the model could be improved by introducing a multipath fading submodel that quantifies the disadvantages of using the system in a enclosed space. A real scenario validation of the reader coverage and S-ALOHA protocol should also be carried out.

Second, we focus on the architectural improvements of the proposed system. Considerations such as creating a mixed-device network (e.g. RFID and mobile) as well as extending the coverage area to other parts of the airport are examples that lie in this group. These would open the door to broaden the scope of the system and include the moments previous to the arrival of passengers at the transit hub (auto industry's "last mile").

Finally, we consider the studies on new applications that take advantage of the massive amount of data generated by this system. A machine learning-based function to detect anomalous trajectories within the terminal or a recommendation system to support personalized advertisement platforms in the airport are examples of projects that can rely on the system we propose.

REFERENCES

[1] D. Bandyopadhyay and J. Sen, "Internet of things: Applications and challenges in technology and standardization," in *Wireless Personal Communications*, vol. 58, no. 1, 2011, pp. 49–69.

[2] G. Bruno and A. Genovese, "A Mathematical Model for the Optimization of the Airport Check-In Service Problem," *Electronic Notes in Discrete Mathematics*, vol. 36, pp. 703–710, aug 2010.

[3] Z. Wu and R. J. Radke, "Real-time airport security checkpoint surveillance using a camera network," in *CVPR 2011 WORKSHOPS*. IEEE, jun 2011, pp. 25–32.

[4] R. O. Mitchell, H. Rashid, F. Dawood, and A. Alkhalidi, "Hajj crowd management and navigation system: People tracking and location based services via integrated mobile and RFID systems," *International Conference on Computer Applications Technology, ICCAT 2013*,

2013.

[5] N. Ishihara, H. Zhao, and R. Shibasaki, "Tracking passenger movement with ground-based laser scanner," in *Paper presented at the 22nd Asian Conference on Remote Sensing*, vol. 5, 2001, p. 9.

[6] P. Falcone, F. Colone, a. Macera, and P. Lombardo, "Localization and tracking of moving targets with WiFi-based passive radar," *Radar Conference (RADAR), 2012 IEEE*, pp. 705–709, 2012.

[7] S. Woo, S. Jeong, E. Mok, L. Xia, C. Choi, M. Pyeon, and J. Heo, "Application of WiFi-based indoor positioning system for labor tracking at construction sites: A case study in Guangzhou MTR," *Automation in Construction*, vol. 20, no. 1, pp. 3–13, 2011.

[8] M. Liem and D. M. Gavrila, "Multi-person tracking with overlapping cameras in complex, dynamic environments," *Procedings of the British Machine Vision Conference 2009*, no. January, pp. 87.1–87.10, 2009.

[9] T. Zhang, Y. Yin, D. Yue, X. Wang, and G. Yu, "Research and implementation of an rfid simulation system supporting trajectory analysis," *Journal of Software*, vol. 9, no. 1, pp. 162–168, 2014.

[10] G. Brookner, "RFID device tracking and information gathering," 2005.

[11] G. E. Vastianos, D. M. Kyriazanos, O. E. Segou, S. A. Mitilineos, and S. C. A. Thomopoulos, "Indoor localization using passive RFID," I. Kadar, Ed., may 2011, p. 80501R.

[12] G. E. Vastianos, D. M. Kyriazanos, V. I. Kountouriotis, and S. C. A. Thomopoulos, "An RFID-based luggage and passenger tracking system for airport security control applications," I. Kadar, Ed., jun, p. 90911A.

[13] A. Kovach, "Method for tracking and processing passengers and their transported articles."

[14] T. McCoy, "RFID for airport security and efficiency," in *IEE Seminar on Signal Processing Solutions for Homeland Security*. IEE, pp. 8–8.

[15] K. Finkenzeller, *RFID handbook: fundamentals and applications in contactless smart cards, radio frequency identification and near-field communication*. John Wiley & Sons, 2010.

[16] M. Buettner and D. Wetherall, "An Empirical Study of UHF RFID Performance," *MobiCom*, pp. 223–234.

[17] Kin Seong Leong, Mun Leng Ng, and P. Cole, "Positioning Analysis of Multiple Antennas in a Dense RFID Reader Environment," in *International Symposium on Applications and the Internet Workshops (SAINTW'06)*. IEEE, pp. 56–59.

[18] R. Want, "An Introduction to RFID Technology," *IEEE Pervasive Computing*, no. 1, pp. 25–33, jan.

[19] M. Sanchez Net, I. del Portillo, B. G. Cameron, E. F. Crawley, and D. Selva, "Integrated tradespace analysis of space network architectures," *Journal of Aerospace Information Systems*, vol. 12, no. 8, pp. 564–578, 2015.

[20] N. Doshi and R. Moriyama, "Application of simulation models in airport facility design," in *Simulation Conference, 2002. Proceedings of the Winter*, vol. 2, 2002, pp. 1725–1730 vol.2.

[21] J. Yanbing, W. Aihua, and C. Haiying, "Simulation and optimization for the airport passenger flow," in *2007 International Conference on Wireless Communications, Networking and Mobile Computing, WiCOM 2007*, 2007, pp. 6599–6602.

[22] A. Verbraeck and E. Valentin, "Simulation building blocks for airport terminal modeling," in *Simulation Conference, 2002. Proceedings of the Winter*, vol. 2. IEEE, 2002, pp. 1199–1206.

[23] W. W. K. Hoeger, L. Bond, L. Ransdell, J. M. Shimon, and S. Merugu, "One-mile step count at walking and running speeds," *ACSM's Health and Fitness Journal*, vol. 12, no. 1, pp. 14–19, 2008.

[24] Ka Keung Lee, Maolin Yu, and Yangsheng Xu, "Modeling of human walking trajectories for surveillance," in *Proceedings 2003 IEEE/RSJ International Conference on Intelligent Robots and Systems (IROS 2003) (Cat. No.03CH37453)*. IEEE, pp. 1554–1559.

[25] R. Boulic, N. M. Thalmann, and D. Thalmann, "A global human walking model with real-time kinematic personification," *The Visual Computer*, no. 6, pp. 344–358, nov.

[26] L. Bezault, R. Boulic, N. Magnenat-Thalmann, and D. Thalmann, "An interactive tool for the design of human free-walking trajectories," *Computer Animation92*, pp. 87–104, 1992.

[27] M. R. Gatersleben and S. W. der Weij, "Analysis and simulation of passenger flows in an airport terminal," in *Simulation Conference Proceedings, 1999 Winter*, vol. 2. IEEE, 1999, pp. 1226–1231.

[28] P. Hart, N. Nilsson, and B. Raphael, "A Formal Basis for the Heuristic Determination of Minimum Cost Paths," *IEEE Transactions on Systems Science and Cybernetics*, no. 2, pp. 100–107.

[29] R. de Neufville, *Airport Systems Planning*. London: Palgrave Macmillan UK.

[30] C. Floerkemeier and S. Sarma, "RFIDSim - A physical and logical layer simulation engine for passive RFID," *IEEE Transactions on Automation Science and Engineering*, vol. 6, no. 1, pp. 33–43, 2009.

[31] D. Arnitz, "Tag Localization In Passive UHF RFID," Ph.D. dissertation, Graz University of Technology, 2011.

[32] Daeyoung Kim, M. Ingram, and W. Smith, "Measurements of small-scale fading and path loss for long range RF tags," *IEEE Transactions on Antennas and Propagation*, no. 8, pp. 1740–1749, aug.

[33] P. Nikitin and K. Rao, "Performance limitations of passive UHF RFID systems," *2006 IEEE Antennas and Propagation Society International Symposium*, pp. 1011–1014, 2006.

[34] A. Bekkali, H. Sanson, and M. Matsumoto, "RFID indoor positioning based on probabilistic RFID map and Kalman Filtering," in *3rd IEEE International Conference on Wireless and Mobile Computing, Networking and Communications, WiMob 2007*, 2007.

[35] K. H. Chen, J. H. Yen, J. H. Tarng, and C. F. Yang, "A low-profile dipole RFID tag antenna with lateral omnidirectional radiation properties for cold-chain logistics applications," *IEEE Antennas and Propagation Society, AP-S International Symposium (Digest)*, pp. 1522–1523, 2014.

[36] S. Kibria, M. T. Islam, and B. Yatim, "New compact dual-band circularly polarized universal RFID reader antenna using ramped convergence particle swarm op-

timization," *IEEE Transactions on Antennas and Propagation*, vol. 62, no. 5, pp. 2795–2801, 2014.

[37] "Alien Technology," http://www.alientechnology.com.

[38] M. S. Daskin, *Network and discrete location: models, algorithms, and applications*. John Wiley & Sons, 2011.

[39] Q. Guan, Y. Liu, Y. Yang, and W. Yu, "Genetic Approach for Network Planning in the RFID Systems," *Sixth International Conference on Intelligent Systems Design and Applications (ISDA '06)*, pp. 567–572.

[40] M. Mitchell, *An introduction to genetic algorithms*. MIT press, 1998.

[41] L. Raisanen and R. M. Whitaker, "Comparison and evaluation of multiple objective genetic algorithms for the antenna placement problem," *Mobile Networks and Applications*, vol. 10, no. 1, pp. 79–88, 2005.

[42] Su-Ryun Lee, Sung-Don Joo, and Chae-Woo Lee, "An enhanced dynamic framed slotted ALOHA algorithm for RFID tag identification," in *The Second Annual International Conference on Mobile and Ubiquitous Systems: Networking and Services*. IEEE, pp. 166–172.

[43] H. Vogt, "Efficient Object Identification with Passive RFID Tags," pp. 98–113.

[44] A. Tanenbaum, *Computer Networks*, 4th ed. Prentice Hall Professional Technical Reference, 2002.

[45] R. V. Levine and A. Norenzayan, "The Pace of Life in 31 Countries," *Journal of Cross-Cultural Psychology*, vol. 30, no. 2, pp. 178–205, 1999.

[46] B. J. Mohler, W. B. Thompson, S. H. Creem-Regehr, H. L. Pick, and W. H. Warren, "Visual flow influences gait transition speed and preferred walking speed," *Experimental Brain Research*, vol. 181, no. 2, pp. 221–228, 2007.

[47] E. Crawley, B. Cameron, and D. Selva, *System architecture: Strategy and product development for complex systems*. Prentice Hall Press, 2015.

BIOGRAPHY

Juan Jose Garau Luis *is a visiting student in the Department of Aeronautics and Astronautics at MIT. Juan Jose received two degrees in Industrial Engineering and Telecommunications Engineering from Universitat Politecnica de Catalunya. He previously worked as a researcher at Barcelona Supercomputing Center and Universitat de les Illes Balears. His research interests focus on the architecture of connectivity systems, RFID and Artificial Intelligence.*

Dr. Marc Sanchez Net *is currently a telecommunications engineer at the Jet Propulsion Laboratory. Prior to this job, he completed his PhD and MS in the department of Aeronautics and Astronautics at MIT. His research focuses on architecting space communication networks to support future space exploration activities, with specific emphasis on the performance of delay tolerant networks at Mars. Prior to MIT, he obtained degrees in both Telecommunications engineering and Industrial engineering from Universitat Politecnica de Catalunya, Barcelona.*

Dr. Bruce Cameron *is a Lecturer in Engineering Systems at MIT and a consultant on platform strategies. At MIT, Dr. Cameron ran the MIT Commonality study, a 16 firm investigation of platforming returns. Dr. Camerons current clients include Fortune 500 firms in high tech, aerospace, transportation, and consumer goods. Prior to MIT, Bruce worked as an engagement manager at a management consultancy and as a system engineer at MDA Space Systems, and has built hardware currently in orbit. Dr. Cameron received his undergraduate degree from the University of Toronto, and graduate degrees from MIT.*

Prof. Edward Crawley *received an Sc.D. in Aerospace Structures from MIT in 1981. His early research interests centered on structural dynamics, aeroelasticity, and the development of actively controlled and intelligent structures. Recently, Dr. Crawley's research has focused on the domain of the architecture and design of complex systems. From 1996 to 2003 he served as the Department Head of Aeronautics and Astronautics at MIT, leading the strategic realignment of the department. Dr. Crawley is a Fellow of the AIAA and the Royal Aeronautical Society (UK), and is a member of three national academies of engineering. He is the author of numerous journal publications in the AIAA Journal, the ASME Journal, the Journal of Composite Materials, and Acta Astronautica. He received the NASA Public Service Medal. Recently, Prof Crawley was one of the ten members of the presidential committee led by Norman Augustine to study the future of human spaceflight in the US.*